

Metadata of the chapter that will be visualized in SpringerLink

Book Title	Geological Evolution of the Precambrian Indian Shield	
Series Title		
Chapter Title	Deformation and Tectonic History of Punagarh Basin in the Trans-Aravalli Terrane of North-Western India	
Copyright Year	2019	
Copyright HolderName	Springer International Publishing AG, part of Springer Nature	
Corresponding Author	Family Name	Bhardwaj
	Particle	
	Given Name	Anamika
	Prefix	
	Suffix	
	Role	
	Division	Department of Earth Sciences
	Organization	Indian Institute of Technology Bombay
	Address	Powai, Mumbai, 400076, India
	Email	anamika.geos@gmail.com
Author	Family Name	Biswal
	Particle	
	Given Name	Tapas Kumar
	Prefix	
	Suffix	
	Role	
	Division	Department of Earth Sciences
	Organization	Indian Institute of Technology Bombay
	Address	Powai, Mumbai, 400076, India
	Email	
Abstract	<p>Trans-Aravalli terrane in the NW India is represented by Neoproterozoic volcano-sedimentary succession of Punagarh Basin that unconformably overlies deformed and metamorphosed basement rocks of Sojat Formation. The basement rocks were deformed into upright inclined folds with parallel to chevron geometry. The axial plane cleavages were developed showing variation in trend from NE-SW to ENE-WSW and this variation was due to late generation open folds. The folded rocks were superimposed by normal as well as strike faults which vary from planar to listric geometry. Due to block rotation roll over antiforms with complimentary synforms were developed. Erinpura granites and Malani Igneous Suite intruded Sojat Formation. Punagrh Group is subdivided into three Formations namely Bambholai Formation, KhamaI Formation and Sowaniya Formation represented by quartzite, shale and bimodal volcanics. The lithological sequence suggests a deposition in a continental rift environment where volcanics were associated with shelf water facies. Normal as well as strike slip faults were developed in the sediments and are syn-kinematic to deposition. While the normal faults strike NE-SW direction the strike slip faults are in WNW-ESE direction. Small scale roll overs, drag folds and flanking structures are associated with normal faults while en-echelon arrays of quartz veins are associated with the strike slip faults. The paleostress tensor analysis of small scale faults suggests a NW-SE extension created normal faults while the strike slip faults were produced from a NNW-SSE compression.</p>	
Keywords (separated by '-')	Punagarh basin - Sojat formation - Normal and strike slip faults - Extensional setting	



Deformation and Tectonic History of Punagarh Basin in the Trans-Aravalli Terrane of North-Western India



Anamika Bhardwaj and Tapas Kumar Biswal

Abstract Trans-Aravalli terrane in the NW India is represented by Neoproterozoic volcano-sedimentary succession of Punagarh Basin that unconformably overlies deformed and metamorphosed basement rocks of Sojat Formation. The basement rocks were deformed into upright inclined folds with parallel to chevron geometry. The axial plane cleavages were developed showing variation in trend from NE-SW to ENE-WSW and this variation was due to late generation open folds. The folded rocks were superimposed by normal as well as strike faults which vary from planar to listric geometry. Due to block rotation roll over antiforms with complimentary synforms were developed. Erinpura granites and Malani Igneous Suite intruded Sojat Formation. Punagrh Group is subdivided into three Formations namely Bambholai Formation, Khamal Formation and Sowaniya Formation represented by quartzite, shale and bimodal volcanics. The lithological sequence suggests a deposition in a continental rift environment where volcanics were associated with shelf water facies. Normal as well as strike slip faults were developed in the sediments and are syn-kinematic to deposition. While the normal faults strike NE-SW direction the strike slip faults are in WNW-ESE direction. Small scale roll overs, drag folds and flanking structures are associated with normal faults while en-echelon arrays of quartz veins are associated with the strike slip faults. The paleostress tensor analysis of small scale faults suggests a NW-SE extension created normal faults while the strike slip faults were produced from a NNW-SSE compression.

Keywords Punagarh basin · Sojat formation · Normal and strike slip faults
Extensional setting

A. Bhardwaj (✉) · T. K. Biswal
Department of Earth Sciences, Indian Institute of Technology Bombay,
Powai, Mumbai 400076, India
e-mail: anamika.geos@gmail.com

Introduction

The North-Western part of Indian shield has preserved a Precambrian geologic history in the form of Aravalli Mountain Ranges and adjoining areas. It has a record of 3500 million years old geological processes and tectonic events. On either side of the Aravalli Mobile belt, there are very large and thick intra-cratonic sedimentary successions of Vindhyan basin in the east and Marwar basin in the west. They are commonly known as the Purana basins having Meso-Neoproterozoic age. Along with these basins the Trans-Aravalli terrain which is a tectono-thermally stable low relief area lying west of Aravalli Mountain Ranges has preserved several isolated volcano-sedimentary basins such as Sirohi basin, Punagarh basin and Sindreth basin, which have different lithopackages and deformation history. The area is mostly covered with tertiary sediments leading to scanty rock outcrops. These basins have recorded late phases of Neoproterozoic crustal evolution of NW Indian shield. Tectonically these basins are different from Purana basins and not much attention has been paid to the detailed structural analysis and understanding deformational history of these basins. Punagarh basin is one such basin where we attempted to deduce the deformational history of the basin in order to understand its significance for tectonic models of Late Precambrian continental evolution.

Regional Geology

The Aravalli-Delhi Mobile belt of the northwestern India depicts a juxtaposition of several terranes along NE-SW trending shear zones which appear as lineaments on the map (Fig. 1 inset). The terranes are namely, Hindoli-Jahajpur Terrane, Mangalwar and Sandmata Terrane, Aravalli Terrane, North Delhi Terrane, South Delhi Terrane and Sirohi Terrane (Singh et al. 2010). The individual Terranes are characterized by distinct sedimentation, deformation, metamorphism and magmatic history. Untala granites, Mewar gneiss, Annasagar gneisses and migmatitic gneisses of Mangalwar and Sandmata Terrane constitute the Archean rocks of the Mobile Belt (ca 3500–2700 Ma, Macdougall et al. 1983; Gopalan et al. 1990; Wiedenbeck and Goswami 1994; Tobisch et al. 1994, Dharma Rao et al. 2011). Collectively these rocks are referred to as the Bhilwara Supergroup and range between ~3500 and 2700 Ma (Gupta et al. 1980; Table 1). The Aravalli Terrane belongs to Paleoproterozoic era and is mostly made of low grade rocks namely basal synrift basic volcanics, stromatolitic phospherite beds, metapelites, dolomites and quartzites (1762 Ma, McKenzie et al. 2013). The Aravalli basin closed at the end of Paleoproterozoic; altered ophiolites bearing Rakhabdev shear zone represents the subduction zone of the Terrane (Deb et al. 1989; Sarkar et al. 1989; Sugden et al. 1990; Verma and Greiling 1995). Synchronous to closing of Aravalli basin, the North Delhi Terrane was developed in form of several isolated basins of quartzite and phyllites around Jaipur, Khetri and New Delhi (~1712, 1854 Ma, Kaur et al.

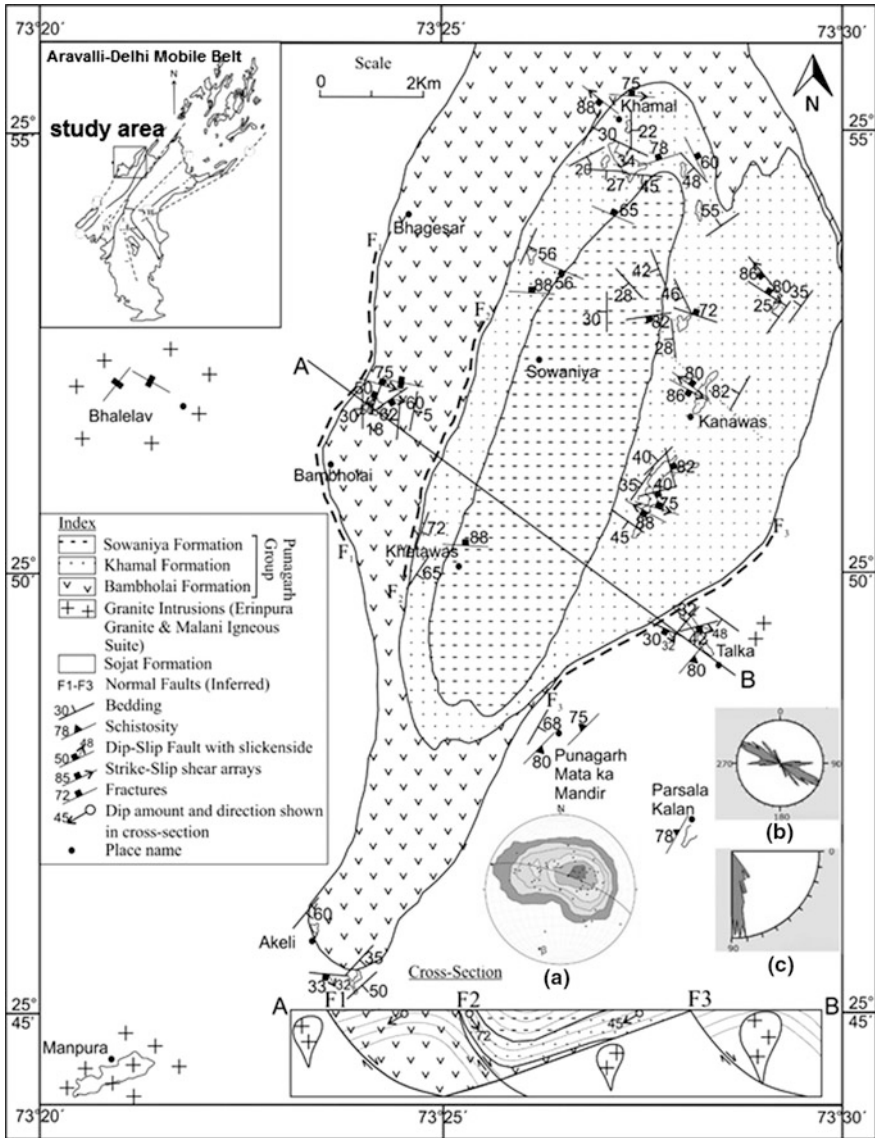


Table 1 Variation in bedding plane dip in Punagarh group rocks

No.	Strike	Dip	Dip direction
1	180	30	W
2	178	35	W
3	185	18	W
4	210	82	NW
5	171	48	W
6	152	43	SW
7	155	46	SW
8	216	17	NW
9	235	50	NW
10	005	28	E
11	000	22	E
12	024	56	SE
13	020	55	SE
14	010	58	SE
15	025	50	SE
16	024	55	SE
17	020	30	SE
18	025	25	SE
19	015	32	SE
20	040	65	SE
21	045	30	SE
22	043	34	SE
23	040	30	SE
24	090	24	S
25	078	32	S
26	040	45	SE
27	045	30	SE
28	080	25	S
29	060	28	SE
30	060	30	SE
31	170	25	W
32	147	35	SW
33	085	28	S
34	062	33	SE
35	290	50	NE
36	145	24	SW
37	095	25	S
38	210	45	NW
39	130	25	SW
40	190	30	W
41	158	42	SW

(continued)

Table 1 (continued)

No.	Strike	Dip	Dip direction
42	125	25	SW
43	112	38	SW
44	138	28	SW
45	138	33	SW
46	155	25	SW
47	175	22	W
48	170	37	W
49	160	25	SW
50	180	30	W
51	180	40	W
52	225	50	NW
53	232	43	NW
54	180	22	W
55	155	30	SW
56	145	40	SW
57	118	35	SW
58	110	45	SW
59	100	50	S
60	138	50	SW

68 [2011, 2013](#)). Contrary to this, the South Delhi Terrane is linear and bears oceanic
 69 signature; it extends from Ajmer to Ambaji and is represented by rift volcanics,
 70 pillowed basalt, extensive Passive Continental Margin deposits (Biswal et al. [1998](#)).
 71 The Terrane opened up in around 1200 Ma (Singh et al. [2010](#)) when rhyolite,
 72 diorite and plagio-granites have been emplaced into the basin (c.a. 1000 Ma, Volpe
 73 and Macdougall [1990](#); Deb and Thorpe [2001](#); Dharma Rao et al. [2013](#)). Phulad
 74 ophiolites represent the obducted oceanic crust. The South Delhi basin closed by
 75 subduction producing island arc in form of Sendra granites, Erinpura granite and
 76 Malani Igneous Suite between 860 and 780 Ma (Crawford [1975](#); Choudhary et al.
 77 [1984](#); Deb and Thorpe [2001](#); Singh et al. [2010](#); Just et al. [2011](#); Meert et al. [2013](#)).
 78 The change over from orogenic cycle of basin evolution and inversion to the phase
 79 of anorogenic magmatism, which is generally bimodal, but dominantly acidic in
 80 character (Bose [1989](#); Bhushan [1995, 2000](#)) along with anorogenic evolution of
 81 ephemeral basins, has been recorded in the Trans-Aravalli terrane. The Sirohi
 82 Terrane occurs to the west of the South Delhi Terrane, in form of isolated outcrops
 83 within vast stretch of Erinpura granites, extending from Sirohi to Sojat and further
 84 north (Tosam). Sirohi Terrane is apparently equivalent in age with the South Delhi
 85 Terrane (Tosam area, 818 and 793 Ma; Murao et al. [2000](#); ~992 and 800 Ma of
 86 granite gneisses, Purohit et al. [2012](#); Dharma Rao et al. [2013](#)). The Sindreth and
 87 Punagarh basins of ~765 Ma age overlie the Sirohi Terrane and Erinpura granites;
 88 these probably constitute part of a back arc basin (Van Lente et al. [2009](#); Dharma

89 Rao et al. 2011). The unmetamorphosed and undeformed volcano-sedimentary
90 succession in the Pali region is described as Punagarh Group. Bimodal volcanism in
91 Punagarh basin marks the onset of anorogenic magmatism.

92 Study Area

93 The Punagarh Group was interpreted as the youngest member of Delhi Supergroup
94 (Gupta et al. 1997; Sinha-Roy et al. 1998; Roy and Jakhar 2002). However, Bose
95 (1989) suggested that these volcano-sedimentary sequences possibly deposited in
96 the time gap between the Delhi Orogeny and the Malani volcanism (Delhi orogeny,
97 ca 850 Ma, Choudhary et al. 1984; Malani Igneous Suite, ca 771–751 Ma; Chore
98 and Mohanty 1998; Torsvik et al. 2001). The Punagarh Group unconformably
99 overlies the Sojat Formation with an angular unconformity at the base. The Sojat
100 Formation is represented by folded and metamorphosed rocks namely slate, phyllite
101 and schist that have been intruded by Erinpura granites and Malani Igneous Suite.
102 However, the Punagarh Group is free from any granitic intrusion. It is subdivided
103 into three formations viz. Bambholai Formation, Khamal Formation and Sowaniya
104 Formation consisting of quartzite, shale and bimodal volcanics. The Punagarh basin
105 evolved as an asymmetric half graben with steeper western flank and outpouring of
106 mafic volcanics of Bambholai Formation was facilitated by these graben related
107 faults (Chore and Mohanty 1998). The Sojat sediments are modeled with Archean
108 gneisses whereas Punagarh group sediments indicate Mesoproterozoic Delhi arc
109 related to back-arc setting based on the provenance analysis using trace elements
110 and petrography (Khan and Khan 2015). A reactivated rift environment (Pali line-
111 eament) in response to a plume activity was suggested for Bambholai volcanics
112 based on the general geology, geochemistry and associated lithology (Khan et al.
113 2004). However, Van Lente et al. (2009) discarded the idea of plume related
114 activity or continental rifting based on the presence of hydrothermally altered
115 basaltic pillow lavas and proposed that low grade alteration features present in the
116 Punagarh basaltic rocks formed as a result of hydrothermal processes associated
117 with basalt–seawater interaction in newly formed oceanic crust favoring a back-arc
118 setting.

119 In this paper we have attempted a large scale mapping of the Punagarh Group
120 and interpretation of structural data. Number of normal faults and strike slip faults
121 has been identified in small to outcrop scale based on brecciation, slickenlines and
122 flanking structure. Based on these small scale structures, we have interpreted large
123 scale structure of the basin. Fault plane analysis has been done using slickenlines
124 and paleostress have been deduced. This helps in understanding the tectonic evo-
125 lution of the trans-Aravalli terrane.

Table 2 Normal fault planes with sliplines (slickensides)

No.	Fault plane		Slickensides	
	Strike	Dip	Trend	Plunge
1	200	50 NW	282	50
2	176	86 W	241	86
3	190	65 W	252	62
4	175	42 W	242	40
5	210	46 NW	272	43
6	022	62 SE	091	61
7	034	70 SE	110	70
8	030	88 SE	120	88
9	020	82 SE	095	82
10	005	88 E	090	88
11	008	75 E	063	72
12	055	75 SE	117	73
13	165	82 E	107	81
14	075	40 SE	140	37
15	045	52 SE	107	49
16	070	46 SE	132	43
17	020	65 SE	081	62
18	038	75 SE	099	73
19	025	70 SE	081	72
20	111	35 SW	191	35
21	114	30 SW	197	30
22	115	28 SW	203	28
23	110	29 SW	197	29
24	108	26 SW	197	26
25	280	26 S	193	26
26	275	35 S	191	35
27	246	54 W	307	50
28	245	47 W	330	47
29	95	33 S	167	32
30	58	54 SE	103	45
31	95	42 N	028	40

Rock Types

- (i) *Basement*: The Sojat Formation is represented by a succession of variegated slate, phyllite, schist, metatuff, sheared quartzite and ferruginous and brecciated quartz rock. The best exposures of Sojat Formation are seen at Sojat fort hill and Punagarh hill. Thick quartz veins are intruded within Sojat slate and phyllite. The schists consist of elongated quartz grains embedded inside biotite matrix. The biotites are aligned parallel to axial plane cleavage of F_1 fold.

Table 3 Conjugate shear planes (conjugate en-echelon quartz vein arrays)

No.	Shear plane 1 (dextral sense of shear)			Shear plane 2 (sinistral sense of shear)		
	Strike	Dip	Dip direction	Strike	Dip	Dip direction
1	100	76	NE	135	85	SW
2	100	78	NE	130	88	SW
3	120	80	NE	150	86	SW
4	120	74	NE	150	82	SW
5	110	70	NE	140	80	SW
6	112	76	NE	145	85	SW
7	120	74	NE	150	85	SW
8	118	80	NE	150	86	SW
9	115	72	NE	155	78	SW
10	110	75	NE	153	88	SW
11	112	78	NE	158	88	SW
12	105	70	NE	135	75	SW
13	100	72	NE	130	78	SW
14	140	70	NE	090	74	SW
15	115	72	NE	138	78	SW
16	105	80	NE	140	84	SW
17	110	74	NE	140	86	SW
18	120	76	NE	148	88	SW

Hence it has been interpreted that a greenschist facies metamorphism has occurred during F_1 stage of folding. Crenulation cleavage has been developed during F_2 folding (Fig. 2a). The other rock type in Sojat Formation is the metatuff that is dark coloured and carries feldspar crystals floating in fine grained matrix. The Sojat rocks are intruded by melanocratic, coarse to medium grained granodiorite at Talka and leucocratic, coarse grained, felsic porphyritic granite near Manpura (Fig. 2b, c respectively). The granodiorite consists of plagioclase, quartz, hornblende, biotite and opaques. The rock has been dated to be ca 800 Ma (Choudhary et al. 1984). The granites are of two types; one abundant with perthite texture and the other lack perthites altogether.

- (ii) *Cover rocks*: Bambholai Formation is the lowest formation in Punagarh Group. It mainly contains pillow basalts with interlayered quartzite and shale beds and it extends from north of Khamal to south of Akeli. Three major lava flows have been delineated based on interflow meta-sediments. The lowermost flow shows few isolated pillows enclosed in subaqueous breccia while upper flows are mostly pillow breccia showing isolated and close packed pillows. The cross-section of pillows is circular to elliptical with a size ranges from 50 cm to 1.5 m. The ratio of longer to shorter axis does not exceed 2.5:1. Undeformed pillows with chilled margins and radial cracks are common. The

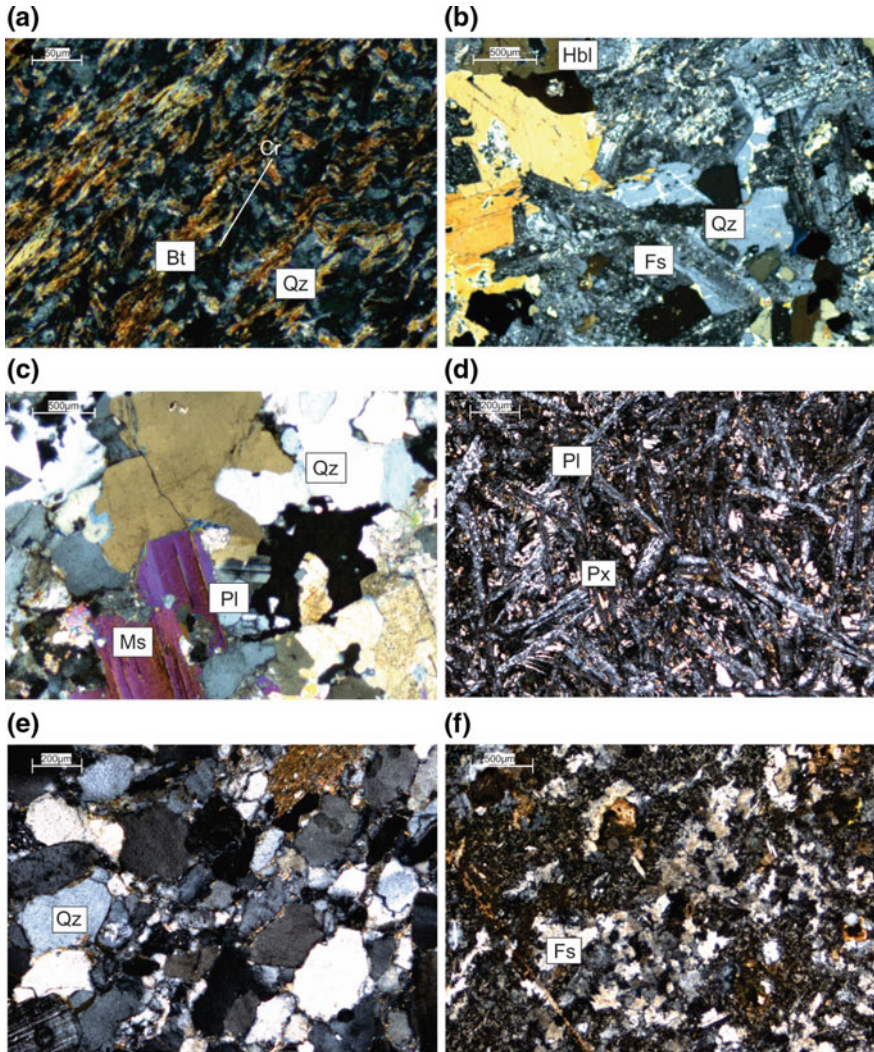


Fig. 2 Photomicrographs, Abbreviations used: Qz—Quartz, Bt—Biotite, Fs—Feldspar, Pl—Plagioclase, Ms—Muscovite, Hbl—Hornblende. **a** Crenulation cleavage (Cr) in Sojat schist, **b** granodiorite intruded in Sojat Formation, **c** granite intruded in Sojat Formation, **d** basalt of Bambholai Formation, **e** quartzite of Khamal Formation, **f** dacite of Khamal Formation

154
155
156
157
158
159

aphanitic lower flow with numerous hyaloclastic bands is separated from middle flow by a thin band of grey jaspery quartzite. Vesicles and amygdules of variable size and shape are common. Basalt shows porphyritic, hyalophitic, intergranular and intersertal texture. Basalt is highly altered to some clay minerals. Minor relict magmatic compositions are preserved. Olivine and plagioclase occur as phenocrysts. Large slender plagioclase laths often

160 showing flow texture are embedded in an altered groundmass containing fine
161 plagioclase microlites. The interspaces created by plagioclase laths are filled
162 with glass, iron oxide (Fig. 2d). Quartzite carries angular to sub-rounded
163 grains with large volume of argillaceous matrix. This indicates low maturity.
164 The Khamal Formation is dominated by quartzite with interbedded chert, shale
165 and dacitic flows. Greenish grey quartzite contains rounded to sub-rounded
166 quartz in siliceous matrix suggesting higher maturity (Fig. 2e). Lithic frag-
167 ments of about 1 cm in size are ubiquitous. Vesicular and amygdule structures
168 are common in dacitic flows. Dacite shows intergranular texture and contains
169 plagioclase laths in a quartzo-feldspathic groundmass (Fig. 2f). Sowaniya
170 Formation mainly comprises fine to medium grained clastics represented by
171 shale, gritty quartzite and metabasic syn-sedimentational flows. Quartzite
172 contains subrounded lithic clasts of shale and slate. Subrounded to subangular
173 quartz with kaolinised feldspar is present in arenaceous matrix of quartzite
174 with minor sphene, epidote and calcite. The syn-depositional mafic and felsic
175 volcanic flows are represented by basalt and rhyolite respectively. Basalt has
176 often preserved pillow structure with a size of an individual pillow varying
177 from 0.5 to 2 m across. Basalt shows hyalophitic texture with large
178 oligoclase-andesine laths present in the altered glassy groundmass. Alteration
179 is a common feature. Well preserved banding and vesicular structures are often
180 observed in interlayered rhyolite. Rhyolite contains euhedral phenocrysts of
181 quartz and feldspar in a fine grained groundmass. Shale exhibits different
182 colors as irregular patches or streaks. Punagarh group of rocks have been
183 intruded by several mafic and felsic dykes. Large hornblende crystal derived
184 from partly alteration of clinopyroxene partially enclosed plagioclase laths
185 giving sub-ophitic to ophitic texture to the dolerite. Felsic dykes which are
186 rhyolitic in composition contain phenocrysts of feldspar in fine grained
187 groundmass.

188 Deformation Structures

- 189
- 190 (i) *Basement rocks*: The Sojat Formation has been deformed into small scale tight
191 isoclinal fold and axial plane cleavage developed parallel to these folds in
192 N75E/42SE direction (Fig. 3a). Later these folds have been superimposed by
193 upright inclined folds with crenulation cleavage having trend that varies from
194 N30E/75NW to N30E/85SE (Fig. 3b) Further the rocks have been faulted by
195 many normal listric as well as normal slip faults (Fig. 3c). Deformation in
196 hanging wall of listric faults led to the development of roll over antiforms
197 (Fig. 3d). Roll over antiforms has produced complimentary synforms. At
198 Punagarh hill, ferruginous brecciated quartzite is developed along a N20E/
199 65SE trending normal fault. At Sinla, the rocks are deformed into sheared
200 quartzite along a N30E/65W trending normal fault where down dip

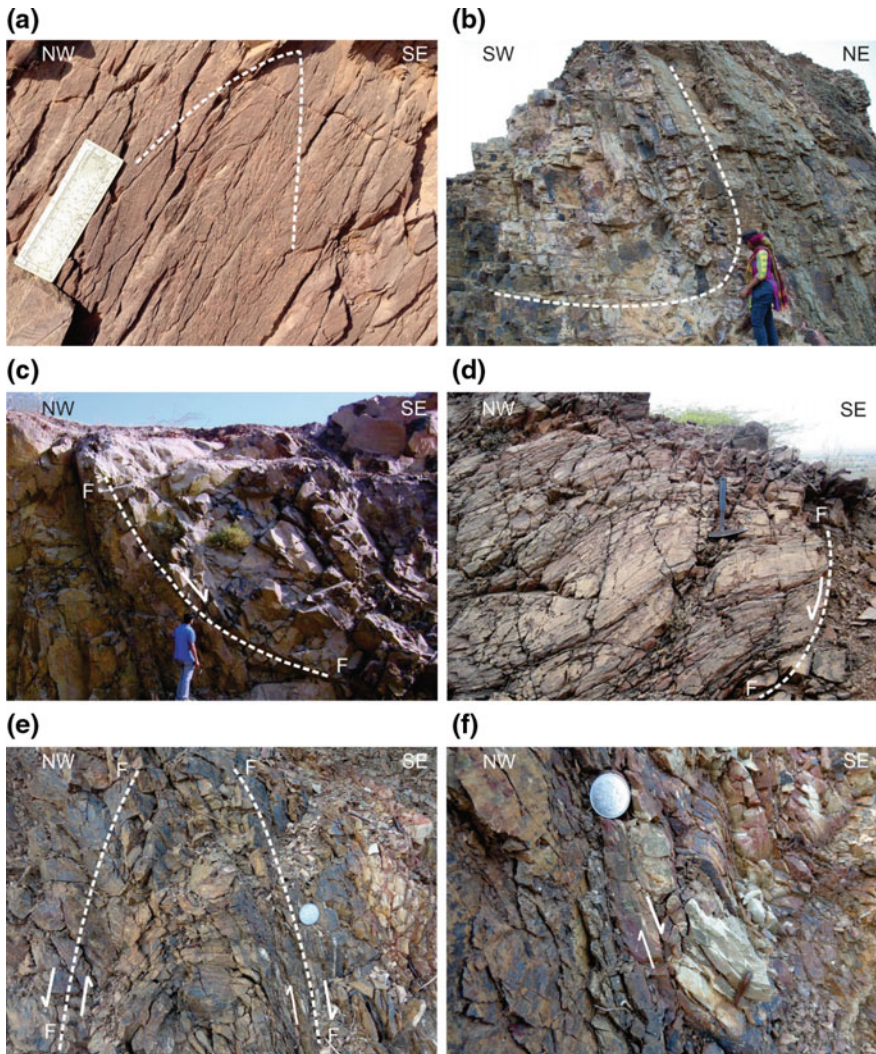


Fig. 3 Structures in Sojat Formation seen on vertical section. **a** Tight isoclinal fold having axial plane dip $N42^{\circ}/345$ within slates, **b** open folds in phyllite at Talika, **c** listric fault with a normal slip, **d** roll over antiform. Structures in Bambholai Formation, **e** antiform structure developed between two normal faults showing opposite sense of shear, **f** shear band defined by fractured rocks between two shear bands flanking structures are observed

201 slickensides are observed. In addition to normal slip faults, strike slip faults are
202 also abundantly developed in the quartzite and schists. The strike of such
203 faults varies from $N110E$ to $N140E$. They behave both in brittle and ductile
204 manner showing both sinistral and dextral sense of shear.

- 205
206 (ii) *Cover rocks*: Punagarh basin shows variation in dip of beds from west to east
207 (Fig. 1) and the variation are shown in equal area projection diagram (Fig. 1a).
208 The fold axis is NE-SW trending with a gentle plunge towards south. This
209 forms a synformal structure within the Punagarh basin. These beds have been
210 transversed by numerous sub-vertical normal faults having NE-SW strike.
211 Near Bambholai shale beds are highly sheared with shear band, brittle S-C
212 structures, antiformal folds and flanking structure (Fig. 3e). The rocks along
213 the shear band are highly fractured and appear almost steep dipping to west as
214 well to east. Between two fault planes, the shale has been dragged along
215 fractures developed due to brittle shearing and thus antiformal structures were
216 formed. These fractures are associated with shear bands and flanking structures
217 (Fig. 3f) that point to normal slip character. Shear bands are brittle in
218 nature and are at low angle to the fault planes with synthetic sense of shear (R
219 shear). Quartzite beds of Punagarh basin are marked with abundant strike slip
220 shear zones hosting en-echelon quartz vein arrays. Dextral and sinistral vein
221 arrays strike N110E and N140E respectively (Fig. 4a). At very few places the
222 vein arrays are sigmoidal (Fig. 4b). Faulting along sinistral vein arrays is very
223 common. Punagarh basin has been intruded by felsic and doleritic dykes
224 parallel to these sinistral strike slip faults.

225 Paleostress Reconstruction

226 Reduced paleostress tensor determination was made by a numerical method,
227 according to the standard procedures (Angelier 1991, 1994; Dunne and Hancock
228 1994). The inversion is based on the assumption of Bott (1959) that slip on a plane
229 occurs in the direction of the maximum resolved shear stress. Fault and shear plane
230 data were inverted to obtain the four parameters of the reduced stress tensor: the
231 principal stress axes σ_1 (maximum compression), σ_2 (intermediate compression,
232 σ_3 (minimum compression) and the ratio of the principal stress differences
233 $R = (\sigma_2 - \sigma_3)/(\sigma_1 - \sigma_3)$. The latter defines the shape of the stress ellipsoid.
234 These parameters are determined by using successively an improved version of the
235 right dihedral method of Angelier and Mechler (1977), and a four dimensional
236 numeric rotational optimization method, using the TENSOR program (Delvaux
237 1993). The two additional parameters of the full stress tensor are the ratio of
238 extreme principal stress magnitudes (σ_3/σ_1) and the lithostatic load, but these
239 cannot be determined from fault data only. Stress regime defines the type of stress
240 tensor. The stress regime is determined by the nature of the vertical stress axes:
241 extensional when σ_1 is vertical, strike-slip when σ_2 is vertical and compressional
242 when σ_3 is vertical. Inside these three major types, the stress regime also varies in
243 function of the stress ratio (R): radial extension (σ_1 vertical, $0 < R < 0.25$), pure
244 extension (σ_1 vertical, $0.25 < R < 0.75$), transtension (σ_1 vertical, $0.75 < R < 1$ or
245 σ_2 vertical, $1 > R > 0.75$), pure strike-slip (σ_2 vertical, $0.75 > R > 0.25$),

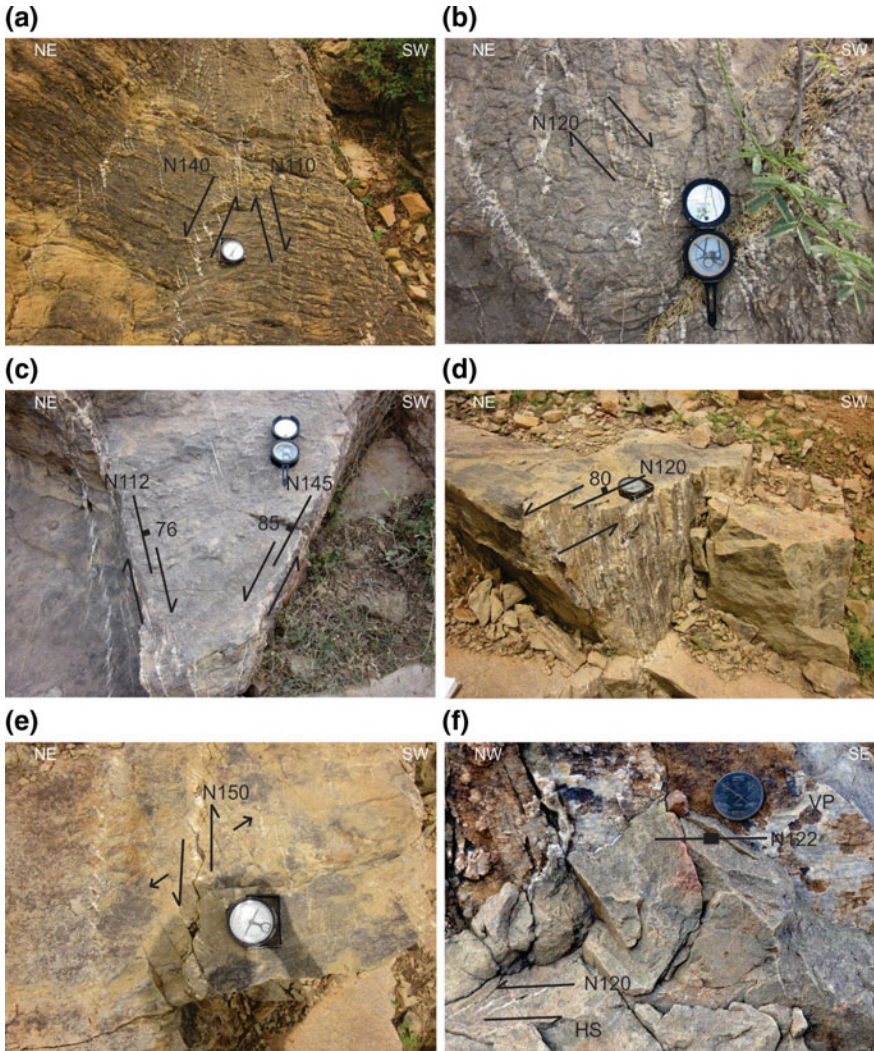


Fig. 4 **a** Strike-slip conjugate set of en-echelon arrays in quartzite of Punagarh group (horizontal section), **b** sigmoidal vein geometry in a sub-horizontal section, **c** fractures along the strike slip shear zones seen in a horizontal section, **d** fracture along the strike slip shear zone seen in a vertical section, **e** strike slip shear along with tension seen on horizontal section of a shear zone, **f** slickenlines on vertical fracture plane (VP) are observed. On horizontal section (HS) en-echelon array is observed showing sinistral sense of shear. Slickenlines are parallel to en-echelon array

246 transpression (σ_2 vertical, $0.25 > R > 0$ or σ_3 vertical, $0 < R < 0.25$), pure compression
 247 (σ_3 vertical, $0.25 < R < 0.75$) and radial compression (σ_3 vertical,
 248 $0.75 < R < 1$) (Delvaux et al. 1997).

249 *Normal slip faults:* Small scale normal slip faults are abundantly developed
 250 within Bhambolai Formation and Sojat Formation. 31 such faults have been analyzed
 251 using win-Tensor, software developed by Dr. Damien Delvaux, Royal
 252 Museum for Central Africa, Tervuren, Belgium. The plunge and azimuth of σ_1 , σ_2
 253 and σ_3 axis is 84/278, 04/046 and 05/136 respectively. This suggests that NW-SE

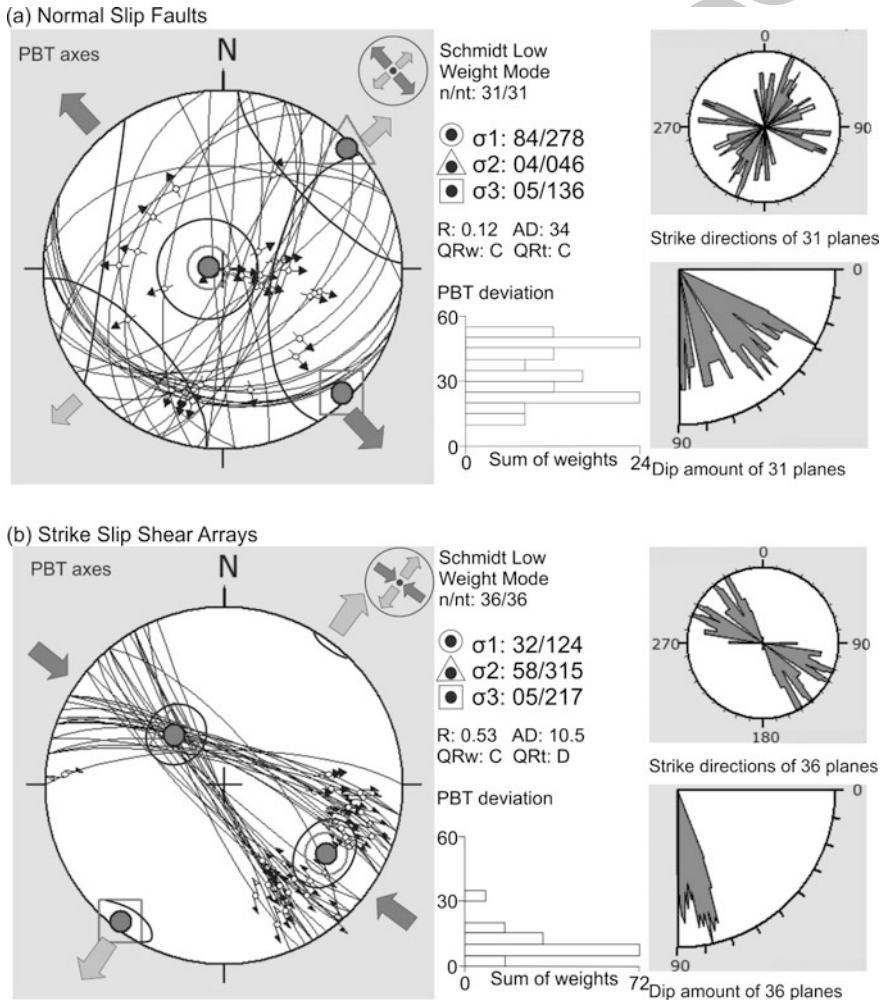


Fig. 5 Paleostress reconstruction for Punagarh basin using Win-Tensor software (Delvaux). **a** Using normal fault planes ($n = 31$), σ_1 : 84/278, σ_2 : 04/046 and σ_3 : 05/136 with $R = 0.12$ suggesting extensional tectonic regime for basin development. Fault plane data has been given in Table 2. **b** Using strike-slip conjugate set of en-echelon arrays of quartz veins ($n = 18$), σ_1 : 32/124, σ_2 : 58/315 and σ_3 : 05/217 with $R = 0.53$ suggesting late phase strike-slip tectonic regime. Strike-slip shear array data given in Table 3. Extension direction during normal faulting and compression direction during strike slip faulting remains same

254 extension has given rise to such faults (Fig. 5a). Radial extensional stress regime is
 255 interpreted from stress ratio ($R = 0.12$).

256 *Strike slip faults:* Fibrous vein systems are normally developed in rocks of
 257 differing competence undergoing deformation in regions of low to middle grade
 258 metamorphism. Fibrous vein systems are generally most abundant in the more
 259 competent layers of a lithologically stratified succession of rocks (Ramsay and
 260 Huber 1983). Numerous arrays of en-echelon quartz filled veins which are aligned
 261 in two intersecting directions and dividing the strained rock mass into wedge
 262 shaped units have been found in quartzite beds of Punagarh basin (Fig. 4a). The
 263 intersection of these en-echelon vein arrays is similar to the patterns formed by
 264 conjugate shear planes. The veins in one array are parallel to the conjugate zone and
 265 interpreted as shear fractures. These conjugate arrays are classified as Type 1 arrays
 266 of Beach (1975). These arrays have been formed during progressive deformation
 267 within established shear zones i.e. the fractures are formed after the shear zone. The
 268 en-echelon vein arrays are classified as transtensional vein arrays because vein
 269 propagate at low angles to the zone ($<45^\circ$) with an accompanying zone dilation and
 270 formation of bridge structures as fracture tips overlap and interact (Beach 1975;
 271 Pollard et al. 1982). At many places, faults have developed along the zones of
 272 en-echelon vein arrays (Fig. 4c, d). Tensional features along with strike slip shear
 273 are also observed in the field showing extension in NNE-SSW (Fig. 4e). Sinistral
 274 sense of shear across the fault plane is inferred from the en-echelon arrays parallel
 275 to fault planes with slickenlines (Fig. 5f). Conjugate arrays of en echelon veins are
 276 one of the kinematic indicators. Mesofracture analysis for the determination of
 277 stress or strain trajectories has been extensively studied by Hancock (1985). It is
 278 assumed that all the sub-vertical to vertical en echelon vein arrays represented
 279 transcurrent dextral and sinistral shear zones. The average dextral and sinistral
 280 trends were noted and these directions were bisected. The acute and obtuse
 281 bisectors of the dihedral angle between the symmetric shear zones will give the
 282 maximum shortening (maximum compression σ_1) and maximum extension (min-
 283 imum compression σ_3) directions and the zonal intersection will give the inter-
 284 mediate strain and stress axis in a fairly homogeneous and isotropic rock. For sites
 285 with a single set of fault slip data, 10–50 measurements with a mean number 20–30
 286 suggest good quality rank for tensor analysis. A total set of 18 conjugate shear
 287 planes (en echelon arrays) were studied in the cover rocks, and their trends with
 288 their dips are plotted in Fig. 5b. The majority of planes of shearing strain fall into
 289 two groups with strike of N110E and N150E. The average of principal stress axes
 290 direction was calculated on TENSOR program. The plunge and azimuth of σ_1 , σ_2
 291 and σ_3 axis is 32/124, 58/315 and 05/217 respectively. The stress tensor is
 292 strike-slip type with NE-SW direction of extension and NW-SE is the direction of
 293 compression.

Large Scale Structure

Based on the dip variation and presence of small scale faults, the large scale structure of the basin has been interpreted. The large scale structure is displayed in form of a cross section (AB) in Fig. 1. The basin appears like a half graben bounded by basin margin faults. On the basis of sedimentation characteristics it has been interpreted that the basin becomes deeper towards west. Three map scale faults have been marked, namely F1, F2 and F3. F1 and F3 are basin margin faults and dip towards SE. F2 is within basin fault and could be a propagation fault developed during sedimentation in form of trishear proposed by Khalil and McClay (2002). Across F1 and F3, roll over antiforms are developed while across F2, drag folds are developed. Because of these fault related folds the Punagarh Basin appears like a synformal structure on the map. The synform plunges to south. In the map an elliptical pattern has been shown. However, the southern closer is due to topography.

Discussion

The trans-Aravalli region is the detached fragment of Arabian Nubian Shield which accreted with southern and western Indian shield at about ca 860 Ma (Singh et al. 2010). A connection between Punagarh, Sindreth and Malani volcanism had been suggested on geological grounds by Roy and Sharma (1999). Punagarh volcanics are younger than 800 ± 2.4 Ma, the age of mafic tonalite (but normatively it is a quartz monzodiorite) containing about 17% hornblende and chloritized biotite represents the basement upon which the Punagarh lavas were erupted (Van Lente et al. 2009). The evolution of these basins is debatable. Sojat Formation which forms the basement of the Punagarh basin represents the youngest member of Delhi Supergroup. Ductile deformation in the form of open folds in the Sojat Formation marks the culmination of Delhi orogeny. It is followed by Erinpura magmatism which is manifested as intrusive relationship with the Sojat Formation. Van Lente et al. (2009) suggested back arc setting for the Punagah basin. However, the quartzite and the shale formations show higher maturity that may not well supportive of back arc character. Further, Delhi orogeny belongs to 850–830 Ma (Singh et al. 2010) and the basins are much younger. Punagarh Group could be equivalent to Malani Igneous Suite or may represent a time gap between the Erinpura magmatism and Malani volcanism. Our study shows that normal faults are responsible for the development of Punagarh basin. The paleostress analysis of normal faults indicates a NW-SE extension. Hence, extension in above direction produced half graben structures which acted as sedimentary repository. The faults are growth faults and helped in deepening of the basin during deposition. As a result the overlying sediments got faulted and propagated faults are produced. One of the basement faults namely the F2 was reactivated and propagated later in the

333 evolution history, thus producing steeper beds adjoining to it in the form of drag
334 folds. Punagarh basin later was controlled by strike slip tectonics developing
335 NW-SE trending faults. Thus the basin was offset from other basin of
336 Trans-Aravalli terrane. Hence it is isolated from Sindreth and other minor basins.
337 Outpouring of lava took place along the basement faults due to extensional setting.
338 Volcanics of Bambholai and dacites of Khamal Formations are examples of such
339 syn-sedimentary volcanism. Syn-extensional sedimentation would have been
340 focused along the longitudinal axis of the hanging wall synclines, whereas footwall
341 uplift would have produced erosion of the pre rift strata; this resulted in deposition
342 of Sowaniya Formation.

343 Conclusion

344 Detailed field mapping and analysis has demonstrated that the kilometer scale half
345 graben structure that has hosted the Punagarh basin is developed over a
346 granitic-metasedimentary crust. The beds have been folded into a southern plunging
347 syncline due to fault related folding. Extension produced such graben structure; the
348 magmatism is related to extensional setting. Continued NW-SE extension produced
349 strike linkage of the fault system which leads to the formation of asymmetric
350 Punagarh basin. Strike-slip tectonics observed in the form of conjugate shear arrays
351 suggesting NW-SE compression is an indicative of change in stress regime of
352 Punagah basin. From these structures, it is suggested that continental extension
353 subsequent to Delhi Orogeny has produced such basin with volcano-sedimentary
354 sequence which later underwent compression. The abundance of brittle deformation
355 with extension parallel to the Pali lineament suggests that the Punagarh basin
356 probably formed as a result of extension in the Trans-Aravalli terrane by reactiva-
357 tion of faults in Pali lineament.

358 **Acknowledgements** This research was supported by Department of Earth Sciences, Indian
359 Institute of Technology.

360 References

- 361 Angelier, J., & Mechler, P. (1977). Sur une méthode graphique de recherche des contraintes
362 principales également utilisable en tectonique et en séismologie: la méthode des
363 dièdres droits. *Bulletin de la Société géologique de France*, 7(XIX), 1309–1318.
- 364 Angelier, J. (1991). Inversion directe de recherche 4-D: comparaison physique et mathématique de
365 deux méthodes de détermination des tenseurs des paléocontraintes en tectonique de failles.
366 *Compte Rendus de l'Académie des Sciences de Paris*, 312(II), 1213–1218.
- 367 Angelier, J. (1994). Fault slip analysis and paleostress reconstruction. In P. L. Hancock (Ed.),
368 *Continental deformation* (pp. 101–120). Oxford: Pergamon.
- 369 Beach, A. (1975). The geometry of en-echelon vein arrays. *Tectonophysics*, 28(4), 245–263.

- 370 Bhushan, S. K. (1995). Late proterozoic continental growth: Implication from geochemistry of
371 acid magmatic events of West Indian craton. *Journal of the Geological Society of India*, 34,
372 339–354.
- 373 Bhushan, S. K. (2000). Malani rhyolites—a review. *Gondwana Research*, 3, 65–77.
- 374 Biswal, T. K., Gyani, K. C., Parthasarathy, R., & Pant, D. R. (1998). Implications of the
375 geochemistry of the Pelitic Granulites of the Delhi Supergroup, Aravalli Mountain Belt,
376 Northwestern India. *Precambrian Research*, 87, 75–85.
- 377 Bose, U. (1989). Correlation problems of the proterozoic stratigraphy of Rajasthan. *Indian*
378 *Minerals*, 43(3–4), 183–193.
- 379 Bott, M. H. P. (1959). The mechanics of oblique slip faulting. *Geological Magazine*, 96(02), 109–
380 117.
- 381 Chore, S. A., & Mohanty, M. (1998). Stratigraphic and tectonic setting of the Trans-Aravalli
382 Neoproterozoic volcanosedimentary sequences in Rajasthan. *Journal of the Geological Society*
383 *of India*, 51, 57–68.
- 384 Choudhary, A. K., Gopalan, K., & Sastry, C. A. (1984). Present status of the geochronology of the
385 Precambrian rocks of Rajasthan. *Tectonophysics*, 105, 131–140.
- 386 Crawford, A. R. (1975). Rb-Sr age determination for the Mount Abu Granite and related rocks of
387 Gujarat. *Journal of Geological Society of India*, 16, 20–28.
- 388 Deb, M., Thorpe, R. I., Cumming, G. L., & Wagner, P. A. (1989). Age, source and stratigraphic
389 Implication of Pb Isotope data for conformable, sediment-hosted, base metal deposits in the
390 Proterozoic Aravalli-Delhi orogenic belt, Northwestern India. *Precambrian Research*, 43, 1–22.
- 391 Deb, M., & Thorpe, R. I. (2001). Geochronological constraints in the Precambrian geology of
392 Northwestern India and their metallogenic implication. In M. Deb & W. D. Goodfellow (Eds.),
393 *Sediment-hosted lead–zinc sulfide deposit in the Northwestern Indian shield, Proceedings of an*
394 *International Workshop, Delhi-Udaipur, India*, pp. 137–152.
- 395 Delvaux, D. (1993). The TENSOR program for paleostress reconstruction: Examples from the east
396 African and the Baikal rift zones. *Terra Nova*, 5(1), 216.
- 397 Delvaux, D., Moeys, R., Stapel, G., Petit, C., Levi, K., Miroshnichenko, A., et al. (1997).
398 Paleostress reconstructions and geodynamics of the Baikal region, central Asia, Part 2.
399 Cenozoic rifting. *Tectonophysics*, 282(1–4), 1–38.
- 400 Dharma Rao, C. V., Santosh, M., Purohit, R., Wang, J., Jiang, X., & Kusky, T. (2011). LA-ICPMS
401 U–Pb zircon age constraints on the Paleoproterozoic and Neoproterozoic history of the Sandmata
402 Complex in Rajasthan within the NW Indian Plate. *Journal of Asian Earth Sciences*, 42,
403 286–305.
- 404 Dharma Rao, C. V., Santosh, M., Kim, S. W., & Li, S. (2013). Arc magmatism in the Delhi Fold
405 Belt: SHRIMP U–Pb zircon ages of granitoids and implications for Neoproterozoic convergent
406 margin tectonics in NW India. *Journal of Asian Earth Sciences*, 78, 83–99.
- 407 Dunne, W. M., & Hancock, P. L. (1994). Palaeostress analysis of small-scale brittle structures.
408 *Continental Deformation*, 5, 101–120.
- 409 Gopalan, K., Macdougall, J. D., Roy, A. B., & Murali, A. V. (1990). Sm–Nd evidence for 3.3 Ga
410 old rocks in Rajasthan, northwestern India. *Precambrian Research*, 48, 287–297.
- 411 Gupta, S. N., Arora, Y. K., Mathur, R. K., Iqballuddin, P. B., Sahai, T. N., & Sharma, S. B. (1980).
412 Lithostratigraphic map of the Aravalli region. Geological Survey of India.
- 413 Gupta, S. N., Arora, Y. K., Mathur, R. K., Iqballuddin, P. B., Sahai, T. N., & Sharma, S. B. (1997). The
414 Precambrian geology of the Aravalli region, southern Rajasthan and north-eastern Gujarat, India
415 (with geological map, Scale 1:2,50,000). *Memoirs of the Geological Survey of India*, 123, 262.
- 416 Hancock, P. L. (1985). Brittle microtectonics: Principles and practice. *Journal of Structural*
417 *Geology*, 7(3), 437–457.
- 418 Just, J., Schulz, B., de Wall, H., Jourdan, F., & Pandit, M. K. (2011). Monazite CHIME/EPMA
419 dating of Erinpura granitoid deformation: Implications for Neoproterozoic tectono-thermal
420 evolution of NW India. *Gondwana Research*, 19, 402–412.
- 421 Kaur, P., Zeh, A., Chaudhri, N., Gerdes, A., & Okrusch, M. (2011). Archaean to Palaeoproterozoic
422 crustal evolution of the Aravalli orogen, NW India, and its hinterland: The U–Pb and Hf
423 isotope record of detrital zircon. *Precambrian Research*, 187, 155–164.

- 424 Kaur, P., Zeh, A., Chaudhri, N., Gerdes, A., & Okrusch, M. (2013). Nature of magmatism and
425 sedimentation at a Columbia active margin: Insights from combined U–Pb and Lu–Hf isotope
426 data of detrital zircons from NW India. *Gondwana Research*, 23, 1040–1052.
- 427 Khalil, S. M., & McClay, K. R. (2002). Extensional fault-related folding, northwestern Red Sea,
428 Egypt. *Journal of Structural Geology*, 24(4), 743–762.
- 429 Khan, M. S., Raza, M., & Safdar-E-Azam, M. (2004). Bombolai Continental Pillow Lavas
430 (Neoproterozoic) from Trans-Aravalli Region, Pali District, Rajasthan and their Tectonic
431 significance. *Geological Society of India*, 64(6), 803–812.
- 432 Khan, T., & Khan, M. S. (2015). Clastic rock geochemistry of Punagarh basin, trans-Aravalli
433 region, NW Indian shield: Implications for paleoweathering, provenance, and tectonic setting.
434 *Arabian Journal of Geosciences*, 8(6), 3621–3644.
- 435 Macdougall, J. D., Gopalan, K., Lugmair, G. W., & Roy, A. B. (1983). The banded Gneissic
436 complex of Rajasthan, India: Early crust from depleted mantle at ~3.5 AE? *Eos, transactions.*
437 *American Geophysical Union*, 64, 351.
- 438 McKenzie, N. R., Hughes, N. C., Myrow, P. M., Banerjee, D. M., Deb, M., & Planavsky, N.
439 J. (2013). New age constraints for the Proterozoic Aravalli-Delhi successions of India and their
440 implications. *Precambrian Research*, 238, 120–128.
- 441 Meert, J. G., Pandit, M. K., & Kamenov, G. D. (2013). Further geochronological and
442 paleomagnetic constraints on Malani (and pre-Malani) magmatism in NW India.
443 *Tectonophysics*, 608, 1254–1267.
- 444 Murao, S., Deb, M., Takagi, T., Seki, Y., Pringle, M., & Naito, K. (2000). Geochemical and
445 geochronological constraints for tin polymetallic mineralization in Tosham area, Haryana,
446 India. In M. Deb (Ed.), *Crustal evolution and metallogeny in northwestern Indian shield*
447 (pp. 43–442). New Delhi: Narosa Publishing House.
- 448 Pollard, D. D., Segall, P., & Delaney, P. T. (1982). Formation and interpretation of dilatant
449 echelon cracks. *Geological Society of America Bulletin*, 93(12), 1291–1303.
- 450 Purohit, R., Papineau, D., Kröner, A., Sharma, K. K., & Roy, A. B. (2012). Carbon isotope
451 geochemistry and geochronological constraints of the Neoproterozoic Sirohi Group from
452 northwest India. *Precambrian Research*, 220, 80–90.
- 453 Queresby, M. N., & Iqbaluddin. (1992). A review of the geophysical constraints in modelling the
454 gondwana crust in India. *Tectonophysics*, 212, 141–151.
- 455 Ramsay, J. G., & Huber, M. I. (1983). *Strain analysis, the techniques of modern structural geology*
456 (Vol. 1)., Strain Analysis London: Academic Press.
- 457 Roy, A. B., & Sharma, K. K. (1999). Geology of the region around Sirohi town, western
458 Rajasthan—story of Neoproterozoic evolution of the Trans-Aravalli crust. In B. S. Paliwal (Ed.),
459 *Geological evolution of Western Rajasthan* (pp. 19–33).
- 460 Roy, A. B., & Jakhar, S. R. (2002). *Geology of Rajasthan (Northwest India)—Precambrian to*
461 *recent* (p. 421). Jodhpur: Scientific Publishers (India).
- 462 Sarkar, G., Burman, T. R., & Corfu, F. (1989). Timing of continental arc-type magmatism in
463 northwest India: Evidence from U to Pb zircon geochronology. *Journal of Geology*, 97,
464 607–612.
- 465 Singh, Y. K., De Waele, B., Karmarkar, S., Sarkar, S., & Biswal, T. K. (2010). Tectonic setting of
466 the Balaream–Kui–Surpagla–Kengora granulites of the South Delhi Terrane of the Aravalli
467 Mobile Belt, NW India and its implication on correlation with the East African Orogen in the
468 Gondwana assembly. *Precambrian Research*, 183, 669–688.
- 469 Sinha-Roy, S., Malhotra, G., & Mohanty, M. (1998). *Geology of Rajasthan* (p. 278). Bangalore:
470 Geological Society of India.
- 471 Sugden, T. J., Deb, M., & Windley, B. F. (1990). The tectonic setting of mineralisation in the
472 proterozoic Aravalli-Delhi orogenic belt, NW India. In S. M. Naqvi (Ed.), *Precambrian*
473 *continental crust and its Economic Resources* (pp. 367–390). New York: Elsevier.
- 474 Tobisch, O. T., Collerson, K. D., Bhattacharya, T., & Mukhopadhyay, D. (1994). Structural
475 relationship and Sm–Nd isotope systematics of polymetamorphic granitic gneisses and granitic
476 rocks from central Rajasthan, India—implications for the evolution of the Aravalli craton.
477 *Precambrian Research*, 65, 319–339.

- 478 Torsvik, T. H., Carter, L. M., Ashwal, L. D., Bhushan, S. K., Pandit, M. K., & Jamtveit, B. (2001).
479 Rodinia refined or obscured: Palaeomagnetism of the Malani igneous suite (NW India).
480 *Precambrian Research*, 108(3), 319–333.
- 481 Van Lente, B., Ashwal, L. D., Pandit, M. K., Bowring, S. A., & Torsvik, T. H. (2009).
482 Neoproterozoic hydrothermally altered basaltic rocks from Rajasthan, northwest India:
483 Implications for late Precambrian tectonic evolution of the Aravalli Craton. *Precambrian*
484 *Research*, 170, 202–222.
- 485 Verma, P. K., & Greiling, R. O. (1995). Tectonic evolution of the Aravalli orogen (NW India): An
486 inverted proterozoic rift basin? *Geologische Rundschau*, 84, 683–686.
- 487 Volpe, A. M., & Macdougall, J. D. (1990). Geochemistry and isotopic characteristics of mafic
488 (Phulad ophiolite) and related rocks in the Delhi Supergroup, Rajasthan, India: Implications for
489 rifting in the Proterozoic. *Precambrian Research*, 48, 167–191.
- 490 Wiedenbeck, M., & Goswami, J. N. (1994). High precision 207 Pb/206 Pb zircon geochronology
491 using a small ion microprobe. *Geochimica Et Cosmochimica Acta*, 58, 2135–2141.

Author Query Form

Book ID : 464726_1_En

Chapter No : 7



Please ensure you fill out your response to the queries raised below and return this form along with your corrections.

Dear Author,

During the process of typesetting your chapter, the following queries have arisen. Please check your typeset proof carefully against the queries listed below and mark the necessary changes either directly on the proof/online grid or in the 'Author's response' area provided below

Query Refs.	Details Required	Author's Response
AQ1	Please confirm if the inserted country name is correct. Amend if necessary.	
AQ2	Kindly note that references Deb et al. (2001), Khan et al. (2015), Van Lente (2009), Delvaux (1997), Sinha-Roy (1998) and Khalil (2002) have been changed to Deb and Thorpe (2001), Khan and Khan (2015), Van Lente et al. (2009), Delvaux et al. (1997), Sinha-Roy et al. (1998) and Khalil and McClay (2002) so that matches in the list.	
AQ3	Please confirm if the section headings identified are correct.	
AQ4	Please provide volume number and page range for this following reference Gupta et al. (1980).	
AQ5	Reference Quereshy and Iqbaluddin (1992) is given in the list but not cited in the text. Please cite this in text or delete from the list.	

MARKED PROOF

Please correct and return this set

Please use the proof correction marks shown below for all alterations and corrections. If you wish to return your proof by fax you should ensure that all amendments are written clearly in dark ink and are made well within the page margins.

<i>Instruction to printer</i>	<i>Textual mark</i>	<i>Marginal mark</i>
Leave unchanged	... under matter to remain	Ⓟ
Insert in text the matter indicated in the margin	∧	New matter followed by ∧ or ∧ [Ⓢ]
Delete	/ through single character, rule or underline or ┌───┐ through all characters to be deleted	Ⓞ or Ⓞ [Ⓢ]
Substitute character or substitute part of one or more word(s)	/ through letter or ┌───┐ through characters	new character / or new characters /
Change to italics	— under matter to be changed	↙
Change to capitals	≡ under matter to be changed	≡
Change to small capitals	≡ under matter to be changed	≡
Change to bold type	~ under matter to be changed	~
Change to bold italic	≈ under matter to be changed	≈
Change to lower case	Encircle matter to be changed	≡
Change italic to upright type	(As above)	⊕
Change bold to non-bold type	(As above)	⊖
Insert 'superior' character	/ through character or ∧ where required	Υ or Υ under character e.g. Υ or Υ
Insert 'inferior' character	(As above)	∧ over character e.g. ∧
Insert full stop	(As above)	⊙
Insert comma	(As above)	,
Insert single quotation marks	(As above)	ʹ or ʸ and/or ʹ or ʸ
Insert double quotation marks	(As above)	“ or ” and/or ” or ”
Insert hyphen	(As above)	⊖
Start new paragraph	┌	┌
No new paragraph	┐	┐
Transpose	┌┐	┌┐
Close up	linking ○ characters	Ⓞ
Insert or substitute space between characters or words	/ through character or ∧ where required	Υ
Reduce space between characters or words		↑